

ORIGINAL ARTICLE

Classification of PD-L1 expression in various cancers and macrophages based on immunohistocytological analysis

Yoichi Saito^{1,2,3,4}  | Yukio Fujiwara¹  | Yusuke Shinchii^{1,5} | Remi Mito^{1,6} |
Yuji Miura^{1,7}  | Tomoya Yamaguchi⁸  | Koei Ikeda⁵ | Shinji Urakami⁹ |
Yuta Nakashima³  | Takuro Sakagami⁶ | Makoto Suzuki⁵ | Yasuhiko Tabata² |
Yoshihiro Komohara¹ 

¹Department of Cell Pathology, Graduate School of Medical Sciences, Faculty of Life Sciences, Kumamoto University, Kumamoto, Japan

²Laboratory of Biomaterials, Institute for Frontier Life and Medical Sciences, Kyoto University, Kyoto, Japan

³Laboratory of Bioengineering, Faculty of Advanced Science and Technology, Kumamoto University, Kumamoto, Japan

⁴Japan Society for the Promotion of Science, Tokyo, Japan

⁵Department of Thoracic Surgery, Graduate School of Medical Sciences, Faculty of Life Sciences, Kumamoto University, Kumamoto, Japan

⁶Department of Respiratory Medicine, Graduate School of Medical Sciences, Faculty of Life Sciences, Kumamoto University, Kumamoto, Japan

⁷Department of Medical Oncology, Toranomon Hospital, Tokyo, Japan

⁸Department of Cancer Biology, Graduate School of Medical Sciences, Faculty of Life Sciences, Kumamoto University, Kumamoto, Japan

⁹Department of Urology, Toranomon Hospital, Tokyo, Japan

Correspondence

Yukio Fujiwara, Department of Cell Pathology, Graduate School of Medical Sciences, Faculty of Life Sciences, Kumamoto University, Honjo 1-1-1, Chuo-ku, Kumamoto, 860-8556, Japan.
Email: fuji-y@kumamoto-u.ac.jp

Funding information

Japan Society for the Promotion of Science, Grant/Award Number: 18J01441 and 19K07459

Abstract

Programmed death (PD)-1/PD-ligand 1 (PD-L1) antibodies have shown an intense clinical effect in some patients with PD-L1⁺ tumors, and their applications have rapidly expanded to various cancer types with or without the application of new companion diagnostics (CDx) with a lower cutoff value and inclusion of macrophage evaluation. However, the pathological background explaining the difference in the cutoff value remains unknown. To address this, we evaluated tissue array samples from 231 patients with lung adenocarcinoma, 186 with lung squamous cell carcinoma, and 38 with renal cell carcinoma (RCC) who were not receiving PD-1/PD-L1 antibodies to investigate the relationship between PD-L1 expression on tumor cells and CD8⁺ T-cell infiltration in tumor tissues. PD-L1 expression in RCC was clearly lower than that in non-small-cell lung cancer (NSCLC) tissue, whereas CD8⁺ T-cell infiltration was low in all cancers. We next analyzed PD-L1 expression by interferon (α , β , and γ) and LPS stimulation in both macrophages and 41 cancer cell lines derived from various organs and histological types. The PD-L1 expression patterns were classified into three types, which differed depending on each organ or tissue type. Interestingly, NSCLC cell lines showed highly diverse PD-L1 expression patterns compared with RCC cell lines. Conversely, PD-L1 expression was stronger and more prolonged in macrophages than in typical cell lines. Here, we revealed the diversity of the PD-L1 expression patterns in tumor

This is an open access article under the terms of the [Creative Commons Attribution-NonCommercial](https://creativecommons.org/licenses/by-nc/4.0/) License, which permits use, distribution and reproduction in any medium, provided the original work is properly cited and is not used for commercial purposes.

© 2022 The Authors. *Cancer Science* published by John Wiley & Sons Australia, Ltd on behalf of Japanese Cancer Association.

cells and macrophages, demonstrating the pathological and cytological significance of the transition of cutoff values in PD-L1 CDx for PD-1/PD-L1 antibody administration.

KEYWORDS

companion diagnostics, macrophage, non-small-cell lung cancer, PD-L1, renal cell carcinoma

1 | INTRODUCTION

Programmed death-ligand 1 (PD-L1) is widely expressed in tumor cells and infiltrated leukocytes, especially tumor-associated macrophages (TAMs).^{1,2} PD-L1 expression in tumor cells is generally induced by interferon (IFN)- γ secreted from the CD8⁺ T cells that infiltrate tumor tissues. The binding of PD-L1 on tumor cells to PD-1 on CD8⁺ T cells causes CD8⁺ T-cell dysfunction; this is called anergy or exhaustion, which decides immune tolerance in the tumor microenvironment.^{3,4} This tolerance causes tumor progression and severely limits the therapeutic effect of cytotoxic anticancer drugs, resulting in poor prognosis.⁵

Immune checkpoint blockade therapy stimulates the antitumor immune response using PD-1/PD-L1 antibodies and causes dramatic effects in some cancers, such as malignant melanoma and non-small-cell lung cancer (NSCLC).⁶⁻¹⁰ The antibodies theoretically prevent immune tolerance by blocking the binding of PD-1 in CD8⁺ T cells and PD-L1 in tumor cells. It is therefore suggested that PD-L1 expression in tumor cells predicts the therapeutic effect of PD-1/PD-L1 antibody therapy. According to this concept, histological evaluation of PD-L1⁺ tumor cells was carried out using immunohistochemistry (IHC) as the first companion diagnostics (CDx) for the administration of pembrolizumab to patients with NSCLC.¹¹⁻¹³ If the therapeutic mechanism of PD-1/PD-L1 antibodies is to inhibit T-cell inactivation, it is important to evaluate T-cell infiltration in tumor tissues before evaluating PD-L1 expression in tumor cells. However, the efficacy of the antibodies is unclear in both high PD-L1 cases without T-cell infiltration and low-PD-L1 cases with high T-cell infiltration. Furthermore, it is also unclear how many of these cases exist for NSCLC.

As their therapeutic mechanism was thought not to depend on the histological type and primary organ of cancer, the applications of PD-1/PD-L1 antibodies have rapidly expanded for various cancer types with CDx. However, the cutoff value of CDx for PD-L1 in squamous cell carcinoma of the head and neck or esophageal cancer is much lower than that for NSCLC.^{14,15} Furthermore, there is no significant evidence regarding the CDx cutoff value in urothelial carcinoma, renal cell carcinoma (RCC), and gastric cancer.¹⁶⁻¹⁸ Therefore, it is necessary to reveal the differences in the pathological background of these cancer types.

It is known that PD-L1 is expressed in TAMs.² As it is difficult to histologically distinguish PD-L1⁺ TAMs from tumor cells, the accuracy of NSCLC CDx based on the tumor proportion score (TPS), counting only the PD-L1⁺ tumor cell rate, is not sufficient. Therefore, patients who were appropriate candidates for PD-1/PD-L1 antibody

therapy were not selected by previous CDx.¹⁹ To address these issues, current CDx for the administration of pembrolizumab to patients with other cancers was modified to include the combined positive score (CPS), which designated both tumor and immune cells as PD-L1⁺ cells. Similarly, respective counting of PD-L1⁺ tumor cells (notated as TCs) and PD-L1⁺ immune cells (ICs) was carried out as the CDx for administering atezolizumab to patients with NSCLC.²⁰ PD-L1 expressed in TAMs is considered to be involved in immune tolerance in the tumor microenvironment; therefore, only PD-L1⁺ ICs have been approved as the CDx for administering atezolizumab and nab-paclitaxel in triple-negative breast cancer.²¹ However, as there is no detailed comparison of PD-L1 expression between macrophages and tumor cells, the distinction between the two remains unclear.

As PD-1/PD-L1 antibodies are extremely expensive, it is medically and economically urgent to develop an accurate CDx that can comprehensively monitor host tumor immunity, including infiltrated CD8⁺ T cells. However, PD-1/PD-L1 antibodies are becoming more widely used as a combination therapy with chemotherapeutic or molecular targeted agents, without any CDx.²²⁻²⁷ Therefore, it is necessary to further investigate the pathological background of different cancer types.

To address these clinical questions, we here reclassified NSCLC and RCC tissue specimens based on CD8⁺ cell infiltration and PD-L1 expression in tumor cells. In addition, we comprehensively analyzed PD-L1 expression in 41 types of cancer cell lines and human monocyte-derived macrophages to classify PD-L1 expression in each cancer according to histological and cytological characteristics.

2 | MATERIALS AND METHODS

2.1 | Patients

Formalin-fixed paraffin-embedded specimens of primary tumor samples were obtained from 231 patients with lung adenocarcinoma and 186 patients with lung squamous cell carcinoma, who had undergone surgery from 2010 to 2013 (adenocarcinoma) and from 2005 to 2018 (squamous cell carcinoma) at Kumamoto University Hospital. Formalin-fixed paraffin-embedded specimens of primary tumor samples were similarly obtained from 38 patients with RCC who had undergone surgery between 1999 and 2010 at Toranomon Hospital. All patients provided written informed consent in compliance with protocols approved by the Institutional Review Board of Kumamoto University Hospital (approval no. 1174) and Toranomon

Hospital (approval no. 1696). Based on the pathological diagnosis report of each case, the most representative area of the 5mm diameter core containing viable cancer cells was removed from the specimen to prepare tissue microarray.

2.2 | Immunostaining

All serial sections (3 μ m) were stored in a deep freezer (-80°C) until immunostaining. Dako Autostainer Link 48 (Agilent Technologies, Santa Clara, CA, USA) was used for immunostaining of PD-L1 (clone 22C3; Agilent Technologies) and CD8 (clone C8/144B; Agilent Technologies) for clinical CDx. For double immunostaining of CD68 and PD-L1, the sections were immersed in EDTA solution (pH 8.0) and heated in a pressure cooker. The sections were reacted with anti-PD-L1 antibodies (clone SP142; Spring Bioscience, Pleasanton, CA, USA) diluted with Can Get Signal immunostain solution A (TOYOBO, Osaka, Japan). Following incubation with primary antibodies, the samples were incubated with horseradish peroxidase-labeled goat anti-rabbit antibodies (Nichirei Bioscience, Tokyo, Japan). Immunoreactions were visualized using the diaminobenzidine substrate system (Nichirei Bioscience) and then washed with citrate buffer (pH 2.2). The sections were reacted with anti-CD68 antibodies (clone PG-M1; Dako, Glostrup, Denmark) and horseradish peroxidase-labeled goat anti-mouse antibody (Nichirei Bioscience), followed by visualization with HistoGreen (Linaris, Dossenheim, Germany). An isotype-matched rabbit or mouse IgG (Agilent Technologies) was used as a negative control. Two pathologists (YS and YK), who were blinded to sample information, evaluated PD-L1 and CD8 expression. PD-L1 expression in tumor cells was evaluated by TPS based on CDx criteria for pembrolizumab. The extent of CD8⁺ T-cell infiltration into the tumor was evaluated using four independent fields at middle magnification ($\times 20$ magnification objective lens). The percentage of the CD8-stained area was calculated using ImageJ software (<https://imagej.nih.gov/ij/>).

2.3 | Graphs and statistics

The graphs were generated using Prism (GraphPad Software Inc., CA, USA). The individual data are expressed as dots with the mean \pm standard deviation (SD). The number in each category was represented by a bar chart. Table analyses were conducted for statistical significance using the two-sided Fisher's exact test. A *p*-value of less than 0.05 was considered to be statistically significant. The statistical analyses were performed using Prism (GraphPad Software Inc.).

2.4 | Human cancer cell lines

Human cancer cell lines purchased from the ATCC (Manassas, VA, USA), JCRB Cell Bank (Osaka, Japan), or Riken BRC (Ibaraki,

Japan) were cultured in polystyrene dishes (Becton Dickinson, Franklin Lakes, NJ, USA) in RPMI 1640 medium (Fujifilm Wako, Osaka, Japan) or DMEM (Fujifilm Wako) supplemented with 1% penicillin/streptomycin and 10% FBS. Human IFN- α (1000 IU/ml; MSD, Tokyo, Japan), IFN- β (10 ng/ml; Peprotech, East Windsor, NJ, USA), IFN- γ (10 ng/ml; Wako), LPS (10 ng/ml; Sigma-Aldrich, St. Louis, MO, USA), or T-cell culture supernatant (described below) was added during the last 24 h of incubation to induce PD-L1 expression.

2.5 | Human monocyte-derived macrophages (HMDMs) and T cells

RPMI 1640 medium (Fujifilm Wako) supplemented with 1% penicillin/streptomycin (Fujifilm Wako) and 10% FBS was used as the complete culture medium for all cells. PBMCs were isolated from peripheral blood obtained from healthy volunteer donors, who provided written informed consent, via density gradient centrifugation with Lymphoprep (Axis-Shield, Oslo, Norway). Monocytes and T cells were isolated from the PBMCs using a magnetic bead-based isolation procedure (MACS CD14 microbeads, Pan T cell Isolation Kit, columns and separators; Miltenyi Biotec, Bergisch Gladbach, Germany). The monocytes were cultured in polystyrene dishes (Becton Dickinson) in complete medium with M-CSF (50 ng/mL; Fujifilm Wako) for 3–7 days to induce HMDM production. The T cells were cultured in the complete medium with immobilized anti-CD3 (5 μ g/ml; Invitrogen, Waltham, MA, USA) and anti-CD28 antibodies (2 μ g/ml; BioLegend, San Diego, CA, USA) for 3–7 days to obtain the culture supernatant. IFNs, LPS, or the T-cell culture supernatant was added to the HMDMs to induce PD-L1 expression. IAXO-101, synthetic CD14/TLR4 antagonist (25 μ M; Innaxon, Tewkesbury, UK), anti-CD14 antibodies (1.5 μ g/ml; R&D Systems, Minneapolis, MN, USA), or mouse IgG1 isotype control (1.5 μ g/ml; MBL, Aichi, Japan) was added 30 min before adding LPS.

2.6 | Western blotting

Cells were solubilized in 1% NP-40 detergent, and the proteins (5–10 μ g) were electrophoresed on a 10% SDS polyacrylamide gel. The proteins were then transferred to PVDF transfer membranes (Millipore, Burlington, MA, USA), which were cut into pieces and incubated with anti-PD-L1 (clone E1L3N; Cell Signaling Technology, Danvers, MA, USA) or anti- β -actin antibodies (clone C4; Santa Cruz Biotechnology, Dallas, TX, USA). The membranes were then visualized using HRP-conjugated anti-mouse or anti-rabbit IgG antibodies (Thermo Fisher Scientific, Waltham, MA, USA) with Pierce ECL Plus Western Blotting Substrate (Thermo Fisher Scientific). Signals were detected using an Amersham Imager 680 (GE Healthcare, Chicago, IL, USA).

3 | RESULTS

3.1 | Widespread distribution of PD-L1 expression and localized distribution of lymphocyte infiltration in NSCLC

"Innate" or constitutive PD-L1 expression without lymphocytic infiltration was often observed in clinical tissue specimens (Figure S1A). In addition, weak or no expression of PD-L1 ("low response") was also observed, despite relatively strong lymphocyte infiltration. This finding suggests that PD-L1 expression in tumor cells can be typically classified into four types based on the expression mechanism²⁸ (Figure S1B). As the CDx for NSCLC focuses only PD-L1 expression, we measured both PD-L1 and CD8 expression in 231 cases of adenocarcinoma and 186 cases of squamous cell carcinoma by immunostaining to classify them into the four categories. As shown in Figures S2 and S3, there were indeed typical clinical cases classified into the four categories.

By evaluating every section with a TPS of 10%, it was found that PD-L1 expression was distributed in all sections (Figure 1A,B). The percentage of infiltrated CD8⁺ cells in the tumor area was distributed within a range of 10% or less (Figure 1A,B). There were more cases of 0% TPS in adenocarcinoma than in squamous cell carcinoma (61% vs. 39%) (Figure 1C,D). Conversely, there were significantly fewer cases of TPS > 10% in adenocarcinoma than in squamous cell carcinoma (27% vs. 38%; $p = 0.02$) (Table 1; Figure S4A). In addition, there were extremely more cases with CD8 area < 1% in adenocarcinoma than in squamous cell carcinoma (94% vs. 64%) (Figure 1E,F). Interestingly, there were only five (2%) cases of CD8 area $\geq 2\%$ in adenocarcinoma, whereas there were 34 (18%) cases of CD8 area $\geq 2\%$ in squamous cell carcinoma ($p < 0.01$) (Table 1; Figure S4B). These data suggested that both PD-L1 expression and CD8⁺ cell infiltration were significantly higher in squamous cell carcinoma than in adenocarcinoma. However, in both histological types, the distribution of CD8⁺ cell infiltration within the range seemed to be low and limited compared with that of PD-L1 expression.

3.2 | Limited distributions of PD-L1 expression and lymphocyte infiltration in RCC

Administration of PD-1/PD-L1 antibodies has rapidly expanded for other cancers, with a low cutoff for the CDx. In particular, there is no cutoff value for CDx of treatment with pembrolizumab for urothelial carcinoma and with pembrolizumab plus axitinib for RCC.^{16,17} To elucidate the pathological basis for these cutoff values, we analyzed PD-L1 expression and CD8⁺ cell infiltration in 38 cases of RCC by IHC. As shown in Figures S5 and 1G, there were no cases in which both PD-L1 TPS and CD8⁺ cell infiltration were high. TPS was < 20% in all cases and < 10% in 97% of cases in RCC (Figure 1H). Moreover, there were significantly fewer cases of TPS > 10% in RCC than in lung adenocarcinoma and squamous cell carcinoma (3% vs. 27%

and 38%; $p < 0.01$) (Table 1; Figure S6A–C). While one case showed marked CD8⁺ cell infiltration ($9 \leq$ CD8 area % < 10%), all other cases showed little CD8⁺ cell infiltration ($0 \leq$ CD8 area % < 3%) (Figure 1I). There was no significant difference in CD8⁺ cell infiltration between RCC and NSCLC (Table 1; Figure S6D–F). Interestingly, TPS was < 10% even in cases with extremely high CD8⁺ cell infiltration. These results suggested that "innate" PD-L1 expression cases with high PD-L1 TPS without CD8⁺ T-cell infiltration are very rare in RCC. Furthermore, as the PD-L1 expression of RCC was weaker than that of NSCLC, it was unclear whether PD-L1 expression was an "adaptive" response to cytotoxicity by CD8⁺ T cells.

3.3 | Classification of PD-L1 expression in several cancer cell lines based on responsiveness to IFNs

PD-L1 expression in tumor cells varied among several type of cancers, including NSCLC and RCC, and few of these cases had strong CD8⁺ T-cell infiltration. Therefore, most PD-L1 expression in tumor cells is not just an "adaptive" response to IFN- γ secreted by activated T cells (Figure 2A). It is therefore suggested that the histopathological PD-L1 expression pattern may be determined by the characteristics of each cancer type. To reveal the characteristics of PD-L1 expression in tumor cells, we analyzed PD-L1 expression in various cancer cell lines by western blotting. PD-L1 expression in cancer cell lines was also classified as "innate" (constantly positive), "adaptive," and "low response" (constantly negative) patterns based on the response with or without IFN- γ stimulation (Figure 2B). In addition, type 1 IFNs (α , β) and LPS also induced PD-L1 expression in HMDMs, similar to IFN- γ (Figure 2C). To carry out more detailed classification of PD-L1 expression patterns in tumor cells, we next comprehensively analyzed PD-L1 expression in various tumor cell lines using several IFNs and LPS. As shown in Figure 2D, type 1 IFNs also enhanced PD-L1 expression. Furthermore, the reactivity to IFN- γ tended to be stronger than that to type 1 IFNs in the adaptive PD-L1 expression group as in HMDMs. Interestingly, HepG2, PANC-1, KNS62, LK-2, and CaOV3 cells hardly responded to type 1 IFNs, despite responding to IFN- γ . Conversely, all tumor cell lines in the low response group, such as uterus endometrial adenocarcinoma, small-cell lung carcinoma, and most breast cancers, had no PD-L1 expression when stimulated with any IFN. Exceptionally, slight LPS-induced PD-L1 expression was observed in some cancer cell lines, such as bladder urothelial carcinoma (T24 and 5637), esophageal cancer (TE-1), and myxofibrosarcoma (malignant fibrous histiocytoma) (NMFH-1) (Figure 2D). Based on the above results, the PD-L1 expression of each cancer cell line was classified by tissue type and organ (Figure 3). The expression was classified into a group when the PD-L1 expression pattern had a clear tendency (upper light gray group) or diversity (lower dark gray group). Three cell lines showed the same PD-L1 expression pattern in uterus endometrioid carcinoma, breast adenocarcinoma, malignant melanoma, and RCC. However, NSCLC did not show this tendency.

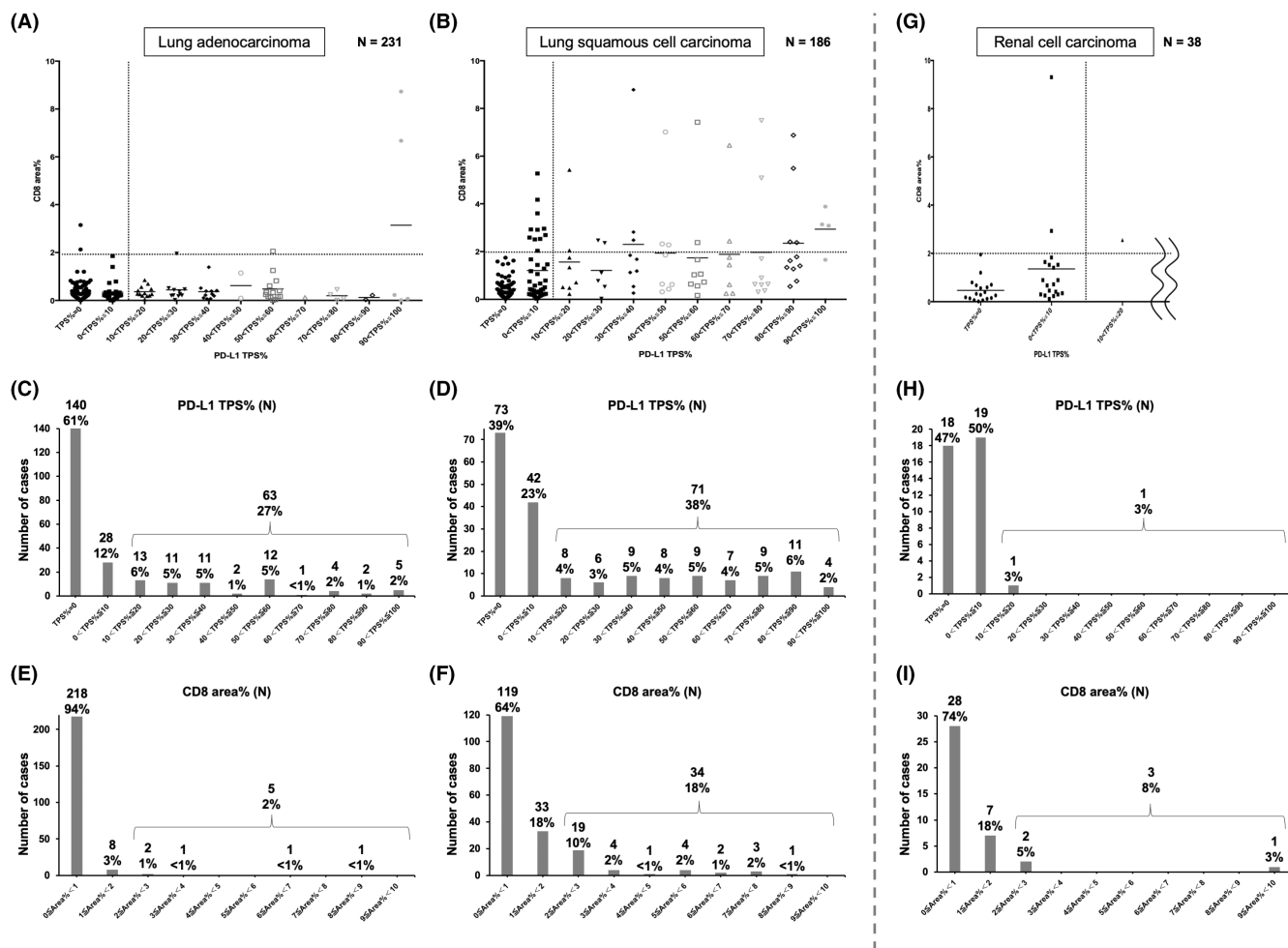


FIGURE 1 Interactions between the PD-L1⁺ tumor cells and CD8⁺ T-cell infiltration in non-small-cell lung cancer (NSCLC) and renal cell carcinoma (RCC). (A, B, G) Correlation distributions of the PD-L1 tumor proportion score (TPS) with tumor-infiltrating CD8⁺ T cells in lung adenocarcinoma (A), squamous cell carcinoma (B), and RCC (G). The groups were classified according to TPS at intervals of 10%, excluding 0%. The percentages of the CD8-stained area (CD8 area %) for each case are displayed as dots and mean bars. (C, D, H) The numbers and proportions of cases for each TPS in lung adenocarcinoma (C), squamous cell carcinoma (D), and RCC (H). (E, F, I) The numbers and proportions of cases for each CD8 area % in lung adenocarcinoma (E), squamous cell carcinoma (F), and RCC (I). The groups were classified according to CD8 area % at intervals of 1% from 0% to 10%

TABLE 1 Associations between cancer type, PD-L1 TPS and CD8⁺ T-cell infiltration analyzed using Fisher's exact test

Cancer type	n	PD-L1 TPS%		p-Value	CD8 area %		p-Value
		≤10	>10		<2	≥2	
Lung adenocarcinoma	231	168	63	0.020	226	5	<0.01
Lung squamous cell carcinoma	186	115	71		152	34	
Lung adenocarcinoma	231	168	63	<0.01	226	5	0.088
Renal cell carcinoma	38	37	1		35	3	
Lung squamous cell carcinoma	186	115	71	<0.01	152	34	0.151
Renal cell carcinoma	38	37	1		35	3	
Non-small-cell lung cancer	417	283	134	<0.01	378	39	1.000
Renal cell carcinoma	38	37	1		35	3	

Note: Bold indicates statistically significant results (*p* < 0.05).

3.4 | Comparison of PD-L1 expression between macrophages and tumor cells

It is difficult to distinguish tumor cells and macrophages by PD-L1 IHC. As shown in Figure 4A,B, PD-L1 was expressed on both tumor cells and TAMs in colorectal cancer tissues, and PD-L1 expression in TAMs was stronger than that in tumor cells. As shown in Figure 2C,D, the typical adaptive PD-L1 expression pattern was observed in HMDMs and the colorectal cancer cell lines, COLO205 and HTC-116. The response to IFN- γ secreted from activated T cells was similar in HMDMs to that observed in COLO205 cells (Figures 2A and 4C), suggesting that T-cell-derived IFN- γ induces PD-L1 expression in both tumor cells and TAMs. The PD-L1 expression in HMDMs with or without IFN- γ -stimulation was stronger than that observed in COLO205 cells (Figure 4D). Furthermore, the duration of IFN- γ -induced PD-L1 expression in HMDMs was markedly longer than that observed in COLO205 cells (Figures 4E,F and 57). These findings indicate that the IFN- γ -induced adaptive PD-L1 expression in TAMs is qualitatively and temporally stronger than that in tumor cells.

3.5 | Macrophage-specific LPS-induced PD-L1 expression via CD14/TLR4 signaling

LPS also strongly induced macrophage-specific PD-L1 expression (Figure 2C,D). The main LPS receptor expressed in macrophages, but not in most tumor cells, was CD14. CD14 activates intracellular signaling pathways by binding to Toll-like receptor 4 (TLR4).²⁹ To reveal the involvement of the pathways in LPS-induced PD-L1 expression in macrophages, the following observations were made after the inhibition experiments. Both the synthetic CD14/TLR4 antagonist IAXO-101 and CD14 antibodies significantly inhibited LPS-induced PD-L1 expression in HMDMs (Figure 5A,B). Furthermore, in cases of bacterial pneumonia, the infiltrating macrophages that were found in an LPS environment highly expressed PD-L1 (Figure 5C). These findings indicated that CD14/TLR4 in macrophages responding to LPS can play a critical role in strong PD-L1 expression in TAMs in outside-opened, nonsterile, and infected tumors.

4 | DISCUSSION

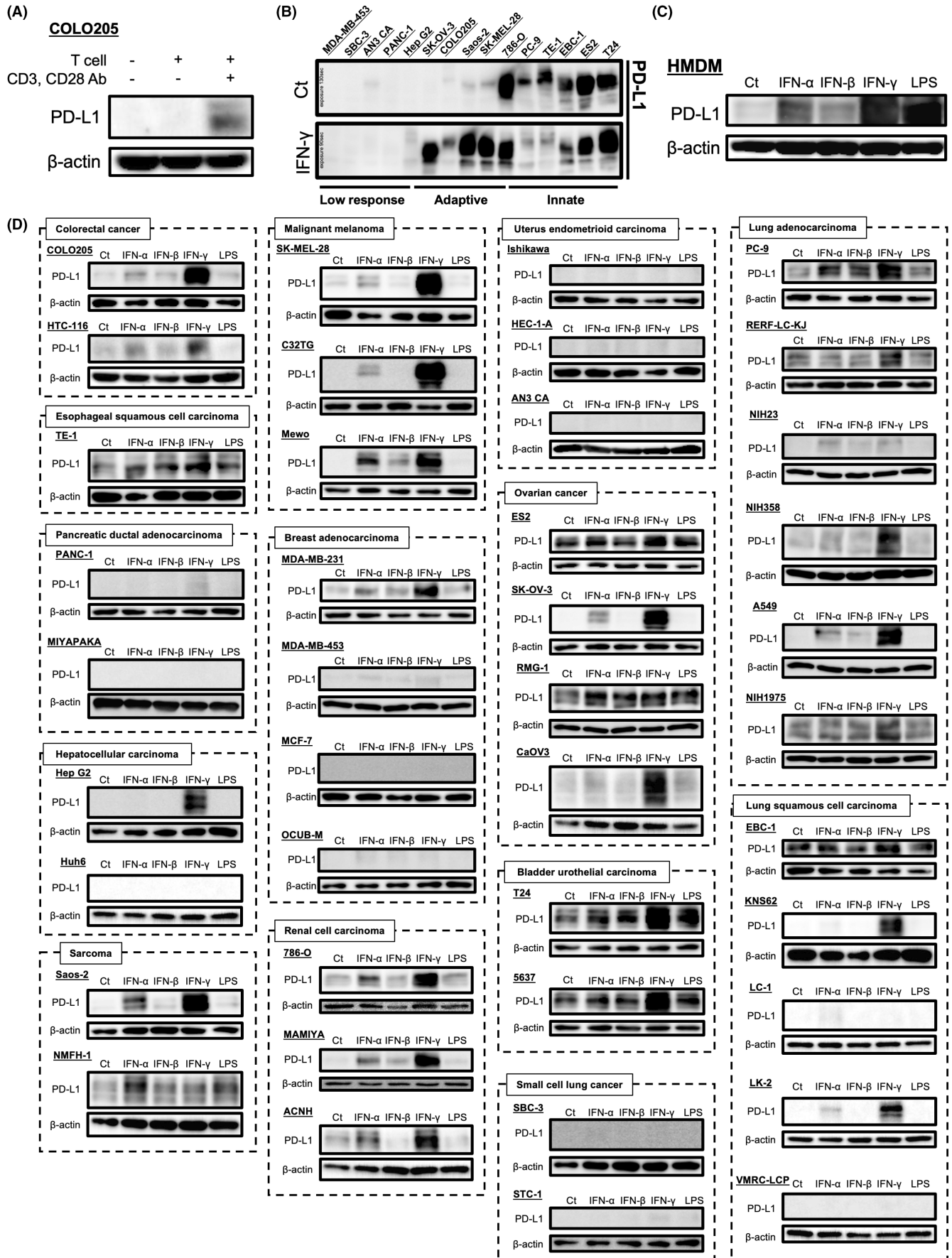
PD-1/PD-L1 antibodies inhibit tumor immunosuppression by blocking the binding of PD-1 in CD8⁺ T cells to PD-L1 in tumor cells.^{4,30} Based on the idea that PD-L1 expression in tumor cells is

a predictive marker of the therapeutic effect of these antibodies, histological evaluation of PD-L1⁺ tumor cells was conducted using IHC as the first CDx for administering pembrolizumab to NSCLC patients.¹³ If the mechanism of these antibodies involves inhibiting T-cell suppression, it is expected that the antibodies will not inhibit T-cell suppression in high PD-L1 cases without T-cell infiltration. It is necessary to evaluate CD8⁺ T-cell infiltration before evaluating PD-L1 on tumor cells in tumor tissue. However, the presence of a high number of cases with PD-L1 expression without T-cell infiltration or with high T-cell infiltration without PD-L1 expression has been confirmed, and the effect of the antibodies in these cases is still unknown. Furthermore, the cutoff values of the CDx of cancers other than NSCLC are much lower than that of NSCLC.^{14,15} To address these clinical questions, NSCLC and RCC tissue specimens were classified into four groups based on CD8⁺ T-cell infiltration and PD-L1 expression in tumor cells (Figures S2, S3 and S5). These data suggested that there are few clinical cases in which PD-1/PD-L1 antibodies would be most effective by targeting CD8⁺ T-cell infiltration, at least at the tissue collection stage. PD-1/PD-L1 antibodies have recently been more widely used with chemotherapeutic or molecular targeted agents as a combination therapy. However, the cutoff values of CDx that are currently being applied clinically are either low or unknown.²²⁻²⁷ It is well known that chemotherapy induces immunogenic tumor cell death and activates tumor-specific T-cell immunity;³¹ these results suggested that chemotherapy can transform adaptive cold tumors into hot tumors, inducing PD-L1 expression in tumor cells attacked by T cells. Therefore, the typical CDx of monotherapy might exclude many patients with adaptive cold tumors that could have induced PD-L1 expression by activating their own T cells.

In addition to IFN- γ , many other factors regulate PD-L1 expression in various cells in the tumor microenvironment.³² However, this does not change the premise that PD-1/PD-L1 antibodies block the binding of PD-1 in CD8⁺ T cells to PD-L1. It is also universally understood that IFN- γ is one of the most robust means by which CD8⁺ T cells damage tumor cells. The differences in PD-L1 expression among the three cancer types explored in this study indicated that their responses to IFN- γ -induced PD-L1 expression are dependent on cancer type. In fact, there were many clinical cases in which PD-L1 expression was unrelated to IFN- γ because of the absence of CD8⁺ T cells (Figure S1A), and there are several reports showing cancers with irregular PD-L1 expression.²⁸ This suggests that the IFN- γ -induced PD-L1 expression pattern should not be underestimated when considering the use of PD-1/PD-L1 antibodies, regardless of cancer type.

Here, by applying the typical classifications shown in Figure S1B, PD-L1 expression in various tumor cell lines was

FIGURE 2 Diversity of IFN-induced PD-L1 expression in various cancer cells. (A) Western blotting analysis of PD-L1 in COLO205 cells cultured with the supernatant of T cells stimulated by immobilized anti-CD3 and anti-CD28 antibodies. (B) Western blotting analyses of PD-L1 in the cultured human cancer cell lines with or without IFN- γ stimulation during the last 24 h of culture. (C) Western blotting analysis of PD-L1 in cultured HMDMs with or without IFN or LPS stimulation during the last 24 h of culture. (D) Western blotting analysis of PD-L1 in 41 cultured human cancer cell lines with or without IFN or LPS stimulation during the last 24 h of culture



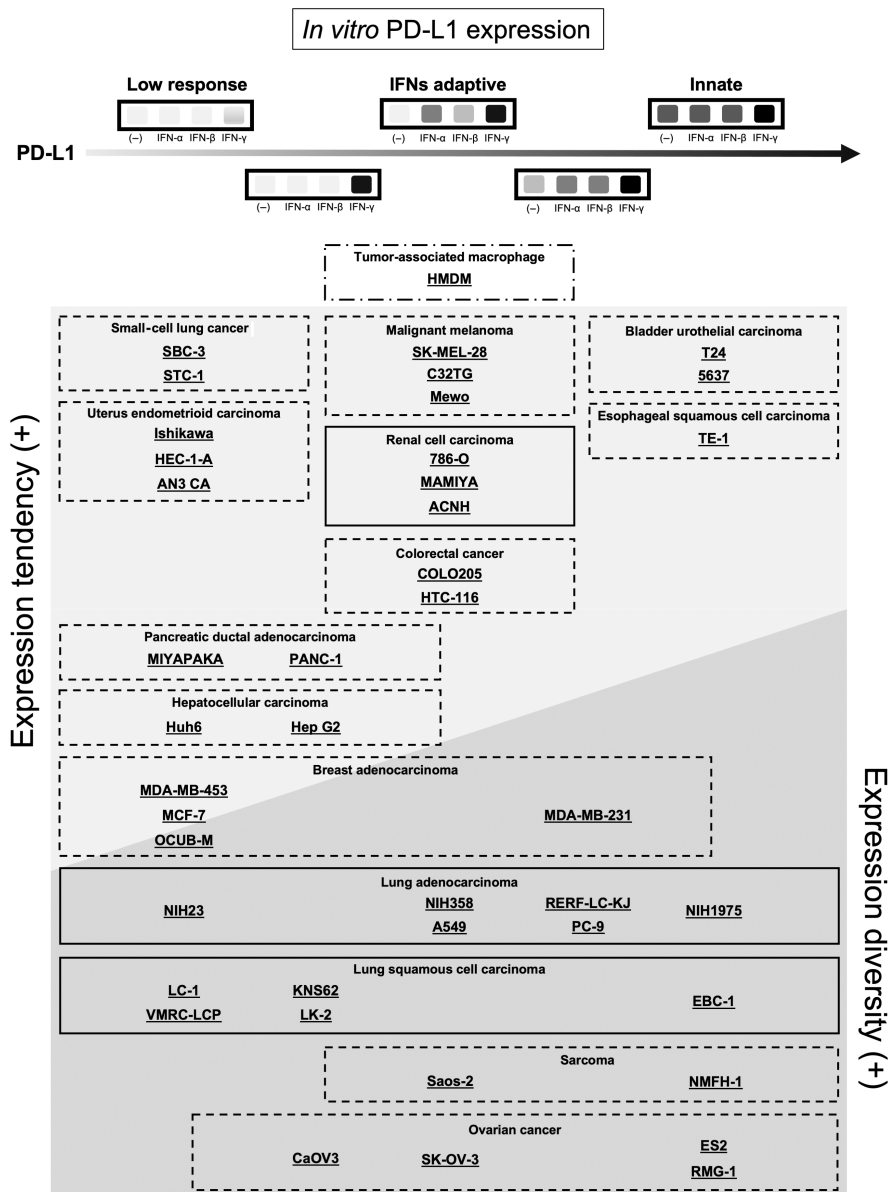
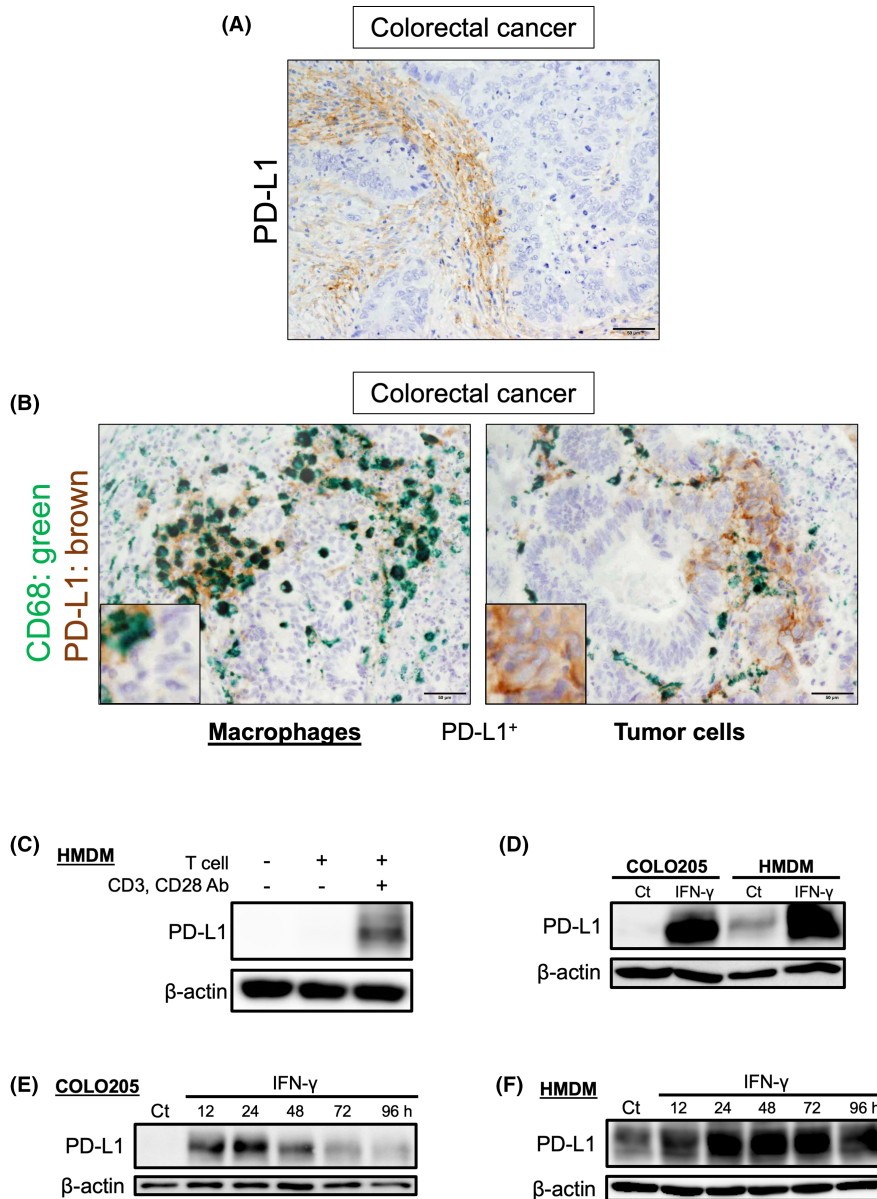


FIGURE 3 Classification of IFN-induced PD-L1 expression in the human cancers and macrophages based on in vitro analysis. PD-L1 expression increases from left to right. The dashed line boxes group the cell lines according to histological type or origin. The highest dashed and dotted box indicates HMDMs. The box width indicates the diversity of PD-L1 expression. The upper, light gray groups have consistent PD-L1 expression. The lower, dark gray groups have diverse PD-L1 expression

classified into three types according to the response to IFN- γ . These categories were "innate" (constantly positive), "adaptive," and "low response" (constantly negative) (Figures 2B and 3). Because IFN- γ can be clinically regarded as a marker for CD8⁺ T-cell infiltration, PD-L1 expression in these cell lines can be summarized as shown in Figure 6A. NSCLC showed an especially high cutoff value for CDx, suggesting that this may be a characteristic population with a diverse PD-L1 expression pattern compared with other cancers, such as RCC, malignant melanoma, or uterus endometrioid carcinoma. Tumor cell lines are a relatively uniform cell population as they are subjected to strong selection pressure during immortalization; in addition, clinical tumors are a collection of tumor cells with diverse characteristics. As such, the discussion of the PD-L1 expression pattern in tumor cell lines certainly has its limitations. However, these data strongly suggest that some cell populations have different PD-L1 expression patterns in clinical

tumors. Therefore, clinical NSCLC is thought to contain all three cell types of PD-L1 expression patterns, as shown in Figure 6B. By contrast, most of clinical RCC cells are considered to be adaptive PD-L1 expression. IHC of clinical specimens of both NSCLC and RCC revealed that CD8⁺ T-cell infiltration was weak in many cases (Figure 1), suggesting that CD8⁺ T cells were not activated or were suppressed by PD-1/PD-L1 signaling or other immune check point molecules (Figure 6C). PD-L1 expression was weak or absent in RCC, an adaptive type of tumor, because of the low number of infiltrated CD8⁺ T cells. However, PD-L1 expression is maintained in NSCLC, which was categorized as having innate expression; these results suggest that this difference in the PD-L1 expression pattern contributes to the difference in its distribution between clinical NSCLC and RCC together with low CD8⁺ T-cell infiltration. The application of PD-1/PD-L1 antibodies for various cancer types is rapidly expanding. However, the cutoff values (CPS, TCs, or ICs)

FIGURE 4 Strong and persistent PD-L1 expression in macrophages compared with that in cancer cells. (A) Immunohistochemistry showed PD-L1 positivity in immune cells and PD-L1 negativity in colorectal cancer cells. Scale bar, 50 μ m. (B) Double immunostaining of PD-L1 and CD68, a pan-macrophage marker, on the tumor sites of colorectal cancer cases. The inner panels indicate higher magnification of cancer cells. Examples of PD-L1 expression in cancer cells are shown with a negative case (left) and a positive case (right). Scale bars, 50 μ m. (C) Western blotting analysis of PD-L1 in HMDMs cultured with the supernatants of T cells stimulated by immobilized anti-CD3 and anti-CD28 antibodies. (D) Comparison of PD-L1 expression in cultured COLO205 cells and HMDMs with and without IFN- γ stimulation during the last 24 h of culture. (E, F) Western blotting analysis of PD-L1 in cultured COLO205 cells (E) and HMDMs (F) with IFN- γ stimulation during the last 12–96 h of culture



are in the range 1–10% for all cancer types except NSCLC. These results indicated that NSCLC may have been incidentally suitable for the CDx and had an unusually high cutoff value (TPS) of 50% because of its cytological features.

We also evaluated PD-L1 expression using type 1 IFNs (α and β) in the tumor cell lines as well as in macrophages (Figure 2C,D). Type 1 IFNs are usually administered systemically or locally to some tumors, such as malignant melanoma or RCC, to damage tumor cells directly.^{33–35} Under similar conditions, PD-L1 expression is likely to be enhanced in cancer cells. The cells damaged by IFN treatment become immunogenic, resulting in the induction of tumor-specific cytotoxic CD8⁺ T-cell infiltration. Therefore, IFN treatment might alter the effect of PD-1/PD-L1 antibodies via activating tumor immunity and enhancing PD-L1 expression in tumor cells.

One important reason for the inadequate accuracy of current CDx is the difficulty in morphologically distinguishing PD-L1⁺ TAMs

from tumor cells (Figure 4A,B). PD-L1 expression in macrophages, which is classified as adaptive, is consistently stronger and more continuous than that in tumor cells (Figures 2C, 4C–F, and S7), suggesting that PD-L1⁺ TAMs should not be excluded in the CDx. Furthermore, several studies also reported that PD-L1⁺ TAMs suppress T-cell activation.^{2,36,37} Therefore, new CDx for squamous cell carcinoma of the head and neck, esophageal cancer, and gastric cancer has been revised to evaluate both PD-L1⁺ tumor cells and TAMs using a CPS.^{14,15,18} Furthermore, the CDx for triple-negative breast cancer was revised to evaluate only PD-L1⁺ lymphocyte, primarily including TAM, as ICs.²¹ As PD-L1 expression is stronger and more continuous in TAMs than in tumor cells, monitoring PD-L1 expression in TAMs may be useful to accurately determine antitumor immunity. The suitability of TPS in NSCLC can be attributed to the high PD-L1 positivity of tumor cells and should be considered to have been specific to NSCLC.

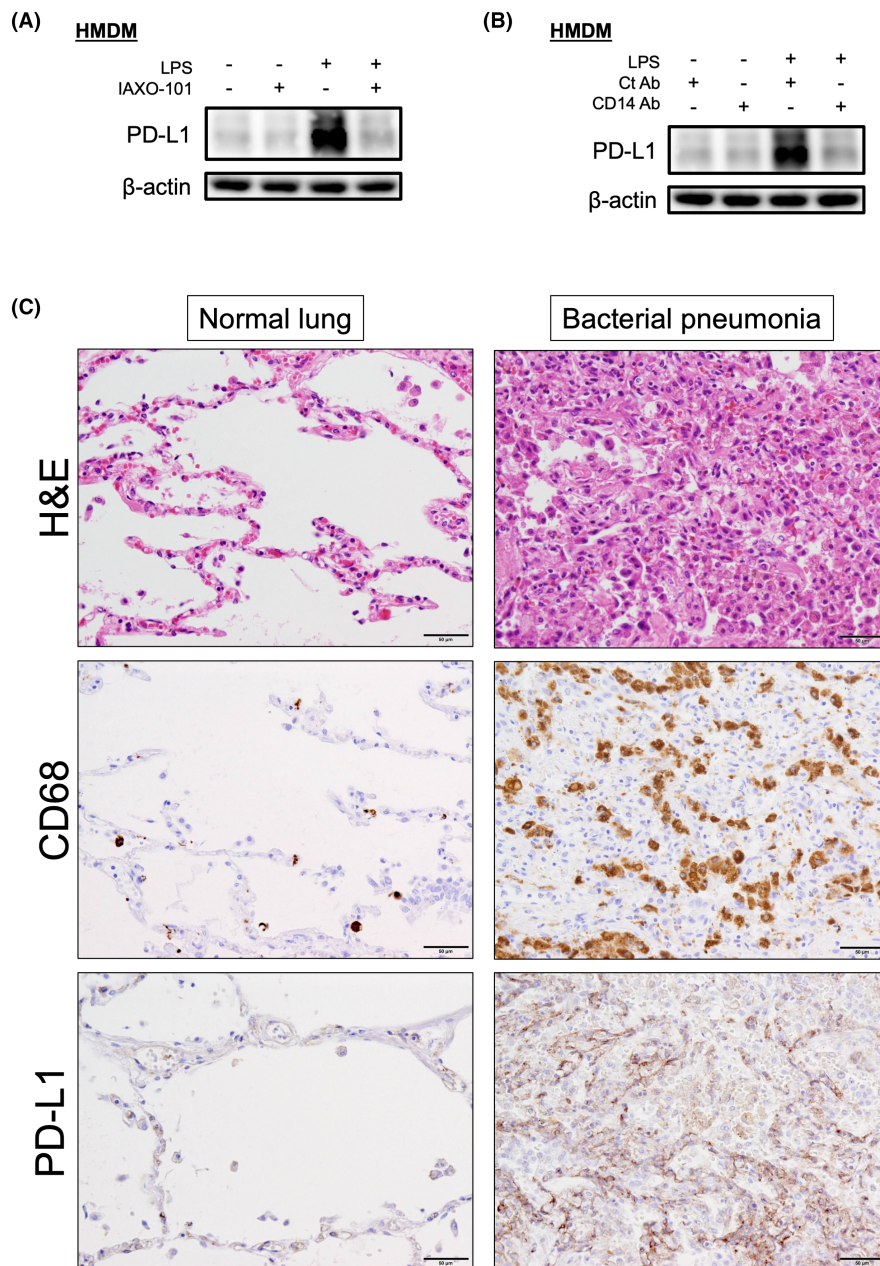


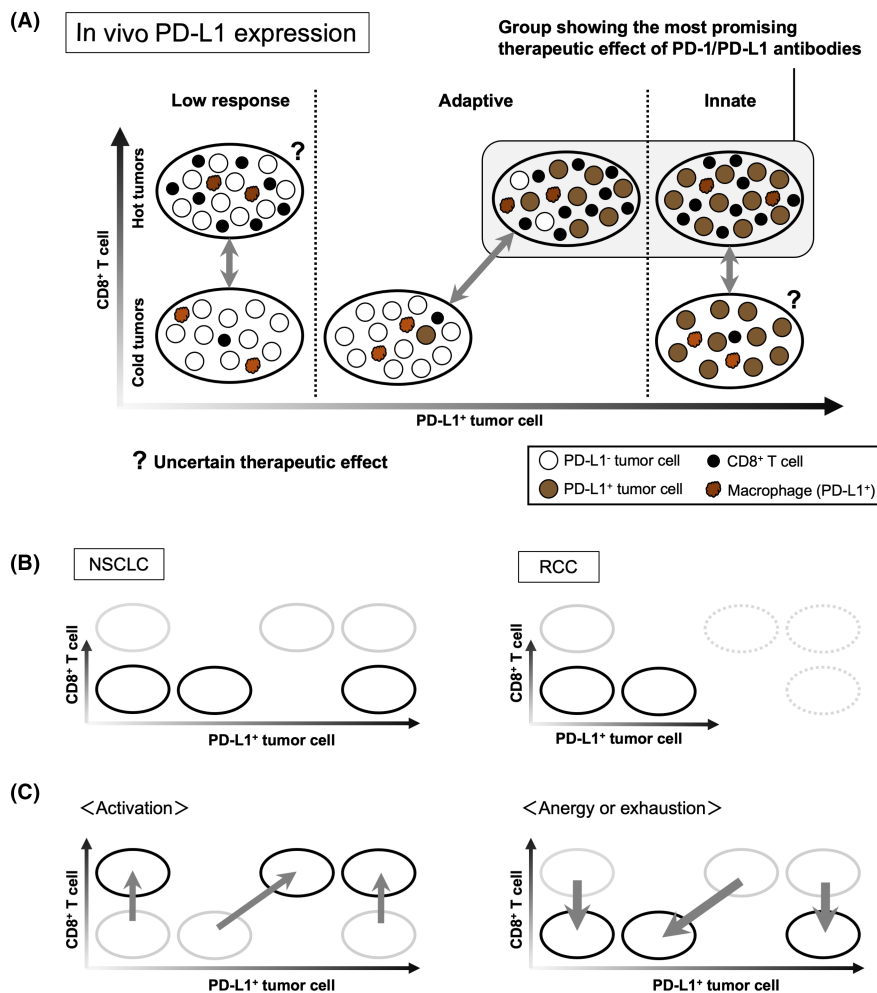
FIGURE 5 Macrophage-specific LPS-induced PD-L1 expression via CD14/TLR4 and increased PD-L1⁺ macrophage infiltration in bacterial pneumonia. (A, B) Western blotting analysis of IFN- γ -induced PD-L1 expression in HMDMs cultured with IAXO-101, synthetic CD14/TLR4 antagonist (A), or anti-CD14 antibodies (B). (C) Hematoxylin and eosin and immunostaining of CD68 and PD-L1 in normal lung and bacterial pneumonia samples. Scale bars, 50 μ m

As shown in [Figure 2C,D](#), LPS strongly induced macrophage-specific PD-L1 expression. The main receptor for LPS is CD14. Furthermore, the binding of CD14 to the coreceptor TLR4 activates intracellular signaling pathways.²⁹ Here, both the synthetic CD14/TLR4 antagonist IAXO-101 and CD14 antibodies significantly inhibited LPS-induced PD-L1 expression in HMDMs ([Figure 5A,B](#)), indicating that CD14 in TAMs plays a critical role in LPS-induced PD-L1 expression at the tumor site. Notably, infiltrated macrophages in bacterial pneumonia strongly expressed PD-L1 ([Figure 5C](#)), providing a potential explanation for the high PD-L1-positive rate of TAMs in organs easily infected with bacteria such as the lung. Although it is unclear whether infection promotes or suppresses the effect of PD-1/PD-L1 antibodies in

patients infected with bacteria receiving the treatment, it is necessary to pay close attention to the change in the therapeutic effect of these antibodies.

In the present study, we classified tumors and macrophages into three types according to the difference in PD-L1 expression patterns and revealed the characteristics of each classification. In addition, an IFN- γ -adaptive PD-L1 expression group mimicked the expression of PD-L1 by macrophages; the PD-L1 expression by macrophages was significantly stronger and longer than that observed in various tumors. Furthermore, we revealed the pathological and cytological significance of cutoff values in PD-L1 CDx for the administration of PD-1/PD-L1 antibodies. Although the therapeutic predictiveness of PD-L1 CDx still remains to be validated in detail, our

FIGURE 6 Improved classification of PD-L1 expression according to CD8⁺ T-cell infiltration in human cancers based on in vivo clinical specimen analysis and in vitro cell line analysis. (A) Circles represent the typical histology of PD-L1 expression and CD8⁺ T-cell infiltration. PD-L1 expression and CD8⁺ T-cell infiltration in tumor cells increase when approaching the right and top of the figure, respectively. The double-headed arrows indicate the possible histological changes. (B) Distributions of the specific histological characteristics of NSCLC and RCC are summarized. (C) Expected changes in PD-L1 expression during immune status



findings regarding the diversity of the PD-L1 expression pattern in tumor cells indicated that it is necessary to develop innovative CDx that can directly monitor tumor immunity.

ACKNOWLEDGMENTS

This study was supported in part by Grants-in-Aid for Scientific Research (18J01441 and 19K07459) from the Ministry of Education, Culture, Sports, Science, and Technology of Japan. This study was also supported in part by a scholarship from the Graduate School of Medical Sciences, Kumamoto University, Japan. We sincerely thank Ms. Ikuko Miyagawa, Ms. Yui Hayashida, Ms. Takana Motoyoshi (K. I. Stainer Inc., Kumamoto, Japan), Mr. Yusuke Izumi, and Mr. Takenobu Nakagawa for their valuable technical assistance. We would like to thank Editage (www.editage.com) for English language editing.

CONFLICT OF INTEREST

The authors declare no competing interests.

DATA AVAILABILITY STATEMENT

The data sets analyzed during the study are available from the corresponding author on reasonable request.

ORCID

Yoichi Saito <https://orcid.org/0000-0001-9097-7656>

Yukio Fujiwara <https://orcid.org/0000-0002-2074-0597>

Yuji Miura <https://orcid.org/0000-0002-7091-628X>

Tomoya Yamaguchi <https://orcid.org/0000-0001-6933-543X>

Yuta Nakashima <https://orcid.org/0000-0003-3151-4963>

Yoshihiro Komohara <https://orcid.org/0000-0001-9723-0846>

REFERENCES

- Okazaki T, Honjo T. PD-1 and PD-1 ligands: from discovery to clinical application. *Int Immunol*. 2007;19:813-824.
- Jiang C, Yuan F, Wang J, Wu L. Oral squamous cell carcinoma suppressed antitumor immunity through induction of PD-L1 expression on tumor-associated macrophages. *Immunobiology*. 2017;222:651-657.
- Dong H, Strome SE, Salomao DR, et al. Tumor-associated B7-H1 promotes T-cell apoptosis: a potential mechanism of immune evasion. *Nat Med*. 2002;8:793-800.
- Blank C, Brown I, Peterson AC, et al. PD-L1/B7H-1 inhibits the effector phase of tumor rejection by T cell receptor (TCR) transgenic CD8⁺ T cells. *Cancer Res*. 2004;64:1140-1145.
- Pardoll DM. The blockade of immune checkpoints in cancer immunotherapy. *Nat Rev Cancer*. 2012;12:252-264.
- Eggermont AMM, Blank CU, Mandala M, et al. Adjuvant pembrolizumab versus placebo in resected stage III melanoma. *N Engl J Med*. 2018;378:1789-1801.

7. Robert C, Long GV, Brady B, et al. Nivolumab in previously untreated melanoma without BRAF mutation. *N Engl J Med*. 2015;372:320-330.
8. Schachter J, Ribas A, Long GV, et al. Pembrolizumab versus ipilimumab for advanced melanoma: final overall survival results of a multicentre, randomised, open-label phase 3 study (KEYNOTE-006). *Lancet*. 2017;390:1853-1862.
9. Brahmer J, Reckamp KL, Baas P, et al. Nivolumab versus docetaxel in advanced squamous-cell non-small-cell lung cancer. *N Engl J Med*. 2015;373:123-135.
10. Borghaei H, Paz-Ares L, Horn L, et al. Nivolumab versus docetaxel in advanced nonsquamous non-small-cell lung cancer. *N Engl J Med*. 2015;373:1627-1639.
11. Reck M, Rodriguez-Abreu D, Robinson AG, et al. Pembrolizumab versus chemotherapy for PD-L1-positive non-small-cell lung cancer. *N Engl J Med*. 2016;375:1823-1833.
12. Herbst RS, Baas P, Kim D-W, et al. Pembrolizumab versus docetaxel for previously treated, PD-L1-positive, advanced non-small-cell lung cancer (KEYNOTE-010): a randomised controlled trial. *Lancet*. 2016;387:1540-1550.
13. Garon EB, Rizvi NA, Hui R, et al. Pembrolizumab for the treatment of non-small-cell lung cancer. *N Engl J Med*. 2015;372:2018-2028.
14. Burtneß B, Harrington KJ, Greil R, et al. Pembrolizumab alone or with chemotherapy versus cetuximab with chemotherapy for recurrent or metastatic squamous cell carcinoma of the head and neck (KEYNOTE-048): a randomised, open-label, phase 3 study. *Lancet*. 2019;394:1915-1928.
15. Kojima T, Shah MA, Muro K, et al. Randomized phase III KEYNOTE-181 study of pembrolizumab versus chemotherapy in advanced esophageal cancer. *J Clin Oncol*. 2020;38:4138-4148. doi:10.1200/jco.20.01888:jco2001888
16. Bellmunt J, de Wit R, Vaughn DJ, et al. Pembrolizumab as second-line therapy for advanced urothelial carcinoma. *N Engl J Med*. 2017;376:1015-1026.
17. Powles T, Plimack ER, Soulières D, et al. Pembrolizumab plus axitinib versus sunitinib monotherapy as first-line treatment of advanced renal cell carcinoma (KEYNOTE-426): extended follow-up from a randomised, open-label, phase 3 trial. *Lancet Oncol*. 2020;21:1563-1573.
18. Shitara K, Van Cutsem E, Bang YJ, et al. Efficacy and safety of pembrolizumab or pembrolizumab plus chemotherapy vs chemotherapy alone for patients with first-line, advanced gastric cancer: the KEYNOTE-062 phase 3 randomized clinical trial. *JAMA Oncol*. 2020;6:1571-1580.
19. Shinchi Y, Komohara Y, Yonemitsu K, et al. Accurate expression of PD-L1/L2 in lung adenocarcinoma cells: a retrospective study by double immunohistochemistry. *Cancer Sci*. 2019;110:2711-2721.
20. Rittmeyer A, Barlesi F, Waterkamp D, et al. Atezolizumab versus docetaxel in patients with previously treated non-small-cell lung cancer (OAK): a phase 3, open-label, multicentre randomised controlled trial. *Lancet*. 2017;389:255-265.
21. Schmid P, Adams S, Rugo HS, et al. Atezolizumab and nab-paclitaxel in advanced triple-negative breast cancer. *N Engl J Med*. 2018;379:2108-2121.
22. Horn L, Mansfield AS, Szczesna A, et al. First-line Atezolizumab plus chemotherapy in extensive-stage small-cell lung cancer. *N Engl J Med*. 2018;379:2220-2229.
23. Gandhi L, Rodriguez-Abreu D, Gadgeel S, et al. Pembrolizumab plus chemotherapy in metastatic non-small-cell lung cancer. *N Engl J Med*. 2018;378:2078-2092.
24. Paz-Ares L, Luft A, Vicente D, et al. Pembrolizumab plus chemotherapy for squamous non-small-cell lung cancer. *N Engl J Med*. 2018;379:2040-2051.
25. Finn RS, Qin S, Ikeda M, et al. Atezolizumab plus Bevacizumab in Unresectable Hepatocellular Carcinoma. *N Engl J Med*. 2020;382:1894-1905.
26. Galsky MD, Ariba JÁA, Bamias A, et al. Atezolizumab with or without chemotherapy in metastatic urothelial cancer (IMvigor130): a multicentre, randomised, placebo-controlled phase 3 trial. *Lancet*. 2020;395:1547-1557.
27. Mittendorf EA, Zhang H, Barrios CH, et al. Neoadjuvant atezolizumab in combination with sequential nab-paclitaxel and anthracycline-based chemotherapy versus placebo and chemotherapy in patients with early-stage triple-negative breast cancer (IMpassion031): a randomised, double-blind, phase 3 trial. *Lancet*. 2020;396:1090-1100.
28. Ribas A, Hu-Lieskova S. What does PD-L1 positive or negative mean? *J Exp Med*. 2016;213:2835-2840.
29. Wu Z, Zhang Z, Lei Z, Lei P. CD14: biology and role in the pathogenesis of disease. *Cytokine Growth Factor Rev*. 2019;48:24-31.
30. Iwai Y, Ishida M, Tanaka Y, Okazaki T, Honjo T, Minato N. Involvement of PD-L1 on tumor cells in the escape from host immune system and tumor immunotherapy by PD-L1 blockade. *Proc Natl Acad Sci USA*. 2002;99:12293-12297.
31. Opzomeer JW, Sosnowska D, Anstee JE, Spicer JF, Arnold JN. Cytotoxic chemotherapy as an immune stimulus: a molecular perspective on turning up the immunological heat on cancer. *Front Immunol*. 2019;10:1654.
32. Kockx MM, McClelland M, Koeppen H. Microenvironmental regulation of tumour immunity and response to immunotherapy. *J Pathol*. 2021;254:374-383.
33. Kilbridge KL, Weeks JC, Sober AJ, et al. Patient preferences for adjuvant interferon alfa-2b treatment. *J Clin Oncol*. 2001;19:812-823.
34. Fujimura T, Okuyama R, Ohtani T, et al. Perilesional treatment of metastatic melanoma with interferon-beta. *Clin Exp Dermatol*. 2009;34:793-799.
35. Mickisch GHJ, Garin A, van Poppel H, de Prijck L, Sylvester R. Radical nephrectomy plus interferon-alfa-based immunotherapy compared with interferon alfa alone in metastatic renal-cell carcinoma: a randomised trial. *Lancet*. 2001;358:966-970.
36. Horlad H, Ma C, Yano H, et al. An IL-27/Stat3 axis induces expression of programmed cell death 1 ligands (PD-L1/2) on infiltrating macrophages in lymphoma. *Cancer Sci*. 2016;107:1696-1704.
37. Umezū D, Okada N, Sakoda Y, et al. Inhibitory functions of PD-L1 and PD-L2 in the regulation of anti-tumor immunity in murine tumor microenvironment. *Cancer Immunol Immunother*. 2019;68:201-211.

SUPPORTING INFORMATION

Additional supporting information may be found in the online version of the article at the publisher's website.

How to cite this article: Saito Y, Fujiwara Y, Shinchi Y, et al. Classification of PD-L1 expression in various cancers and macrophages based on immunohistocytological analysis. *Cancer Sci*. 2022;113:3255-3266. doi: [10.1111/cas.15442](https://doi.org/10.1111/cas.15442)